UNIVERSITY OF PARDUBICE

FACULTY OF CHEMICAL TECHNOLOGY

Department of General and Inorganic Chemistry

Jan Smolík

Photo-induced effects in high-refractive index glasses

Theses of the Doctoral Dissertation

Pardubice 2022

Study Program: **Chemistry and Technology of Materials**

Study field: **Chemistry and Technology of Inorganic Materials**

Author: **Ing. Jan Smolík**

Supervisor: **doc. Ing. Eva Černošková, CSc.**

Supervisor-specialist: **Ing. Petr Knotek, Ph.D.**

Year of the defence: 2022

References

SMOLÍK, Jan. *Photo-induced effects in high-refractive index glasses*. Pardubice, 2022. 135 pages. Dissertation thesis (Ph.D.). University of Pardubice, Faculty of Chemical Technology, Department of General and Inorganic Chemistry. Supervisor doc. Ing. Eva Černošková, CSc. Supervisor-specialist Ing. Petr Knotek, Ph.D.

Abstract

In this thesis, mainly the photo-induced effects formed on the surface of oxide high-refractive index glasses (systems $PbO\text{-}Ga_2O_3$, $PbO\text{-}Bi_2O_3\text{-}Ga_2O_3$ a $PbO\text{-}ZnO\text{-}CoO\text{-}P_2O_5$) were examined. The illumination led generally to the formation of microlenses and also microcraters or microlines in some cases. These microobjects have potential applications in optics. The role of basic parameters influencing the microlenses formation (exposition time, laser power density, chemical composition and structure of glasses) was investigated. Several properties of microlenses from point of potential imaging applications (i.e. optical transmission and ability to display an object, determination of linear refractive index, radius of curvature and focal length) were determined as well. In addition, the all microobjects were characterized using energy dispersive X-ray analysis, Raman spectroscopy and/or nanoindentation. The properties of created microobjects and non-illuminated area were compared. The thermal model using the calculation of temperature rise upon the illumination was used to determine the mechanism of microobjects formation. Finally, the photo-viscous changes, as the effects which influence the formation of microobjects, were studied using thermomechanical analysis in As_2S_3 and selected oxide glass containing Co^{2+} ions.

Keywords

high-refractive index glasses, direct CW laser writing, microlens, microcrater, microline, photo-viscous changes

Abstrakt

V této práci byly zkoumány převážně fotoindukované jevy vytvářené na povrchu oxidových skel s vysokým indexem lomu (systémy $PbO\text{-}Ga_2O_3$, $PbO\text{-}Bi_2O_3\text{-}Ga_2O_3$ a $PbO\text{-}ZnO\text{-}CoO\text{-}P_2O_5$). Působením záření docházelo především k tvorbě konvexních mikročoček, dále pak mikrokráterů či mikrolinií, kdy všechny uvedené mikroútvary nacházejí potenciální uplatnění v optice. Byly zjištěny základní parametry ovlivňující tvorbu mikročoček jako doba expozice, intenzita záření, chemické složení a struktura. Byly popsány některé vlastnosti mikročoček: ověření propustnosti a zobrazování předmětů, určení indexu lomu, poloměru křivosti a ohniskové vzdálenosti. Vytvářené mikroútvary byly charakterizovány pomocí porovnání energiově disperzní rentgenové analýzy, Ramanovy spektroskopie a/nebo nanoindentace s vlastnostmi neosvíceného skla. Pro odhadnutí mechanismu tvorby mikroútvarů byl vytvořen teplotní model, který umožňoval určit lokální ohřev vzorku působením záření. Jako efekt ovlivňující tvorbu mikroútvarů na povrchu skel byly pomocí termomechanické analýzy zkoumány fotoindukované změny viskózního toku v As_2S_3 a vybraném oxidovém skle obsahujícím Co^{2+} ionty.

Klíčová slova

skla s vysokým indexem lomu, přímý zápis kontinuálním laserem, mikročočka, mikrokráter, mikrolinie, fotoviskózní změny

Content

Introduction

Photo-induced effects are formed during the interaction between a material and light with the appropriate photon energy and intensity. These effects are studied especially on the amorphous materials (thin films, bulk samples) where they can be more pronounced due to the lack of long-order arrangement, presence of various defects and larger free volume in comparison with the crystalline materials. The interaction of glass with the suitable light leads in the first step to the absorption of light which can cause the excitation of electrons or holes, displacement of atoms, phonon amplification and/or temperature rise. Consequently, the formation of a new phase or various changes in electronic or atomic structure, chemical composition and/or various properties (e.g. optical, electrical, thermal or mechanical) can occur [1].

Photo-induced effects can be divided according to the effect's time duration into three groups: irreversible (permanent, e.g. [2]), reversible (can be erased by annealing at temperature near glass transition temperature [3] or by illumination using the light with suitable intensity and energy [4]) and transient (observed only upon illumination, e.g. [5]). The most important photo-induced effects are photo-darkening [6], photo-bleaching [7], photo-chromism [8], photo-crystallization [9] and even reversible photo-crystallization/photo-amorphization [10] which all have the various potential applications as optical or electrical devices.

Except the above-mentioned effects, the illumination can lead to the photo-induced material volume changes which can result in the formations of microlenses [11], microcraters [12] or even their arrays [13]. All mentioned microobjects can find potential applications as passive optical elements. The formation of microlenses and microcraters has been studied especially in chalcogenide glasses (e.g. [14-16]) that exhibit typically pronounced photo-sensitivity to wavelengths from the visible region. On the other hand, the formations of these objects have also been extended into some oxide glasses (e.g. [12, 17-21]) mainly due to the development of more intensive lasers (e.g. pulsed lasers) and/or due to the use of lasers emitting in the mid-infrared region.

The photo-induced formation of the microlenses is usually explained by the various mechanisms such as the photo-structural changes [22], local temperature overheating [21] or chemical changes [23]. In the case of microcraters formation due to CW laser illumination, various thermal effects such as increasing viscous flow [24], selective evaporation of volatile compounds [12] or explosive boiling [24] are suggested to be the mechanism of their formation.

It was also suggested (e.g. in [25]) that the photo-induced volume changes could be in some cases connected with the photo-induced viscous flow changes known also as photo-fluidity. Photo-induced viscous flow changes have been examined in some chalcogenide glasses, i.e. Se, As_2S_3, e.g. [25-27]. In the mentioned works, it was assumed that the nature of the observed photo-viscous changes is athermal connected with some transient photo-structural changes (e.g. dynamic weakening of some weak binding interactions in glasses and subsequent rearrangement or formations of some charge defects increasing the mobility of atoms and/or clusters). The light induced viscous flow changes were also observed in phosphate glass $Co(PO_3)_2$ [27] where the observed increase of viscous flow upon illumination was, in contrast to chalcogenides, attributed to the local temperature rise as the result of the non-uniform heating of the sample.

1. High-refractive index glasses – motivation and aims

This thesis focuses on the study of the photo-induced volume changes and microobjects formation (i.e. microlenses, microcraters and microlines) on the surface of selected oxide glasses (i.e. $PbO\text{-}Ga_2O_3$, $PbO\text{-}Bi_2O_3\text{-}Ga_2O_3$ and $PbO\text{-}ZnO\text{-}CoO\text{-}P_2O_5$ systems).

The mentioned glassy systems were selected especially due to the high content of heavy metal oxides which provide certain properties comparable with the chalcogenide glasses. The examined glasses exhibit relatively high the linear and non-linear refractive index [28-30], high value of the coefficient of thermal expansion [30, 31], good transmission in the infrared region [30, 32], and/or relatively low values of glass transition temperature, e.g. [32]. The chemical stability of selected oxide glasses also plays an important role [30, 33].

These materials were also selected because they absorb the light from the visible region due to the high content of PbO, Bi_2O_3 or the presence of Co^{2+} ions. The formation of microobjects on these glasses can therefore be performed using the industrially more widespread and mainly cheaper continuous-wave laser sources emitting visible light (λ = 447 and 532 nm).

The main aims of this thesis are to find the suitable chemical composition of glass, to create microobjects on the surface and to characterize them using the important parameters. The important task is to find the mechanism of their formation taking into account the different light absorption mechanisms (i.e. by short wavelength absorption edge ($PbO\text{-}Ga_2O_3$ and $PbO\text{-}Bi_2O_3\text{-}Ga_2O_3$ glasses) or by d-d transitions of present colorants, Co^{2+} ions in $PbO\text{-}ZnO\text{-}CoO\text{-}P_2O_5$ glasses). The characterization of the created microobjects especially from the point of their potential applicability as the passive optical element (i.e. imaging properties) is also highly desirable. The remaining important task is the comparison of properties of non-illuminated and illuminated surface.

All selected glasses were therefore characterized to obtain the optical and thermal properties which both influence the response of the material to the illumination. The imaging through the microlens was performed and the imaging properties such as linear refractive index of microlens (by Lorentz-Lorenz relation [34]), radius of curvature (r_c) [35] and focal length (f) [35] were calculated.

The thermal model dealing with the local overheating of the sample during the illumination was applied to better understand the response of studied glasses to illumination.

The second part of this work is focused on the study of photo-viscous changes. For these purposes, the modified thermomechanical analyzer enabling the action of the applied force and light in the same direction on the same place of the sample was used. The basic parameters influencing the photo-viscous changes were determined using chalcogenide As_2S_3 glass as the model system due to its high photo-sensitivity (e.g. [25, 27]). The photo-viscous changes of the selected oxide glass with the significantly different structure, optical properties and absorption mechanism were examined and characterized.

The used experimental procedures and the obtained results are described in the following sections.

2. Experimental procedures

2.1 Glasses preparation

In this work, various bulk samples of high-refractive index glasses were selected to study the several photo-induced effects, especially photo-induced microstructuring of glassy surfaces. All glasses were prepared using the conventional melt-quenching technique. Oxide glasses were synthesized using various suitable inorganic compounds (e.g. PbO or H_3PO_4) and each synthesis was performed in a corundum crucible in a crucible furnace with an air access at T ≈ 1050 °C for 15 min to avoid the changes of chemical composition. The corresponding oxide glasses were obtained by cooling the melt poured onto the nickel substrate in the air. In the case of glassy As_2S_3, the synthesis was performed from the corresponding pure elements in evacuated and sealed quartz ampoule at T ≈ 800 °C within 7 hours and the resulting glass was obtained by cooling the ampoule containing the melt in the air.

All prepared glasses were annealed at temperature slightly below their glass transition temperature to remove the stress. The real chemical composition of prepared oxide glasses was determined using EDX or XRF analysis, see Table 1 and 2. In the tables, the abbreviations used further in the text are also listed. The real chemical composition of As_2S_3 was also verified by EDX analysis.

Table 1 *The real chemical composition of the prepared glasses* $(PbO)_x(Ga_2O_3)_{100-x}$, $x = 69.8\text{-}78.9$ *mol%, and* $(PbO)_{75-x}(Bi_2O_3)_x(Ga_2O_3)_{25}$, $x = 3.3\text{-}29.8$ *mol%, detected by EDX and XRF analysis.*

$(PbO)_x(Ga_2O_3)_{100-x}$		$(PbO)_{75-x}(Bi_2O_3)_x(Ga_2O_3)_{25}$	
Composition by EDX	**Abbreviation**	**Composition by XRF**	**Abbreviation**
$(PbO)_{69.8}(Ga_2O_3)_{30.2}$	PG1	$(PbO)_{71.4}(Bi_2O_3)_{3.3}(Ga_2O_3)_{25.3}$	PBG1
$(PbO)_{74.7}(Ga_2O_3)_{25.3}$	PG2	$(PbO)_{67.0}(Bi_2O_3)_{7.6}(Ga_2O_3)_{25.4}$	PBG2
$(PbO)_{76.1}(Ga_2O_3)_{23.9}$	PG3	$(PbO)_{60.0}(Bi_2O_3)_{15.0}(Ga_2O_3)_{25.0}$	PBG3
$(PbO)_{77.3}(Ga_2O_3)_{22.7}$	PG4	$(PbO)_{52.5}(Bi_2O_3)_{22.5}(Ga_2O_3)_{25.0}$	PBG4
$(PbO)_{78.9}(Ga_2O_3)_{21.1}$	PG5	$(PbO)_{45.6}(Bi_2O_3)_{29.8}(Ga_2O_3)_{24.6}$	PBG5

Table 2 *The real chemical composition of the prepared glasses* $((PbO)_{55}(ZnO)_{10}(P_2O_5)_{35})_{100-x}(CoO)_x$, $x = 0\text{-}3.57$ *mol%, determined by XRF analysis.*

Composition by XRF	**Abbreviation**
$(PbO)_{54.92}(ZnO)_{10.04}(P_2O_5)_{35.04}$	PZPCo0
$(PbO)_{54.88}(ZnO)_{10.06}(P_2O_5)_{34.91}(CoO)_{0.15}$	PZPCo1
$(PbO)_{54.08}(ZnO)_{10.43}(P_2O_5)_{35.04}(CoO)_{0.45}$	PZPCo2
$(PbO)_{53.77}(ZnO)_{10.45}(P_2O_5)_{34.88}(CoO)_{0.90}$	PZPCo3
$(PbO)_{53.84}(ZnO)_{9.84}(P_2O_5)_{34.30}(CoO)_{2.02}$	PZPCo4
$(PbO)_{52.55}(ZnO)_{10.17}(P_2O_5)_{33.71}(CoO)_{3.57}$	PZPCo5

2.2 Direct laser writing

The direct laser writing was performed on sample surfaces polished to the optical quality (i.e. roughness expressed as RMS-RR parameter < 0.01λ [36]) using

continuous-wave (CW) lasers emitting at 447 and 532 nm. The laser beams were focused onto the sample surfaces by the constructed optical apparatus (for λ = 447 nm, see Fig. 1) and in the case of λ = 532 nm by the optical microscope which is the part of commercial Raman spectrophotometer Dimension P2 (Lambda Solution, USA). The time of illumination was 0.1-60 s according to the properties of materials. The available laser power densities $F_{L,\,max}$ reached up to 1900 W/cm^2 for 447 nm and 475 W/cm^2 for 532 nm). The thickness of samples was the same in all experiments (1.2 ± 0.1 mm).

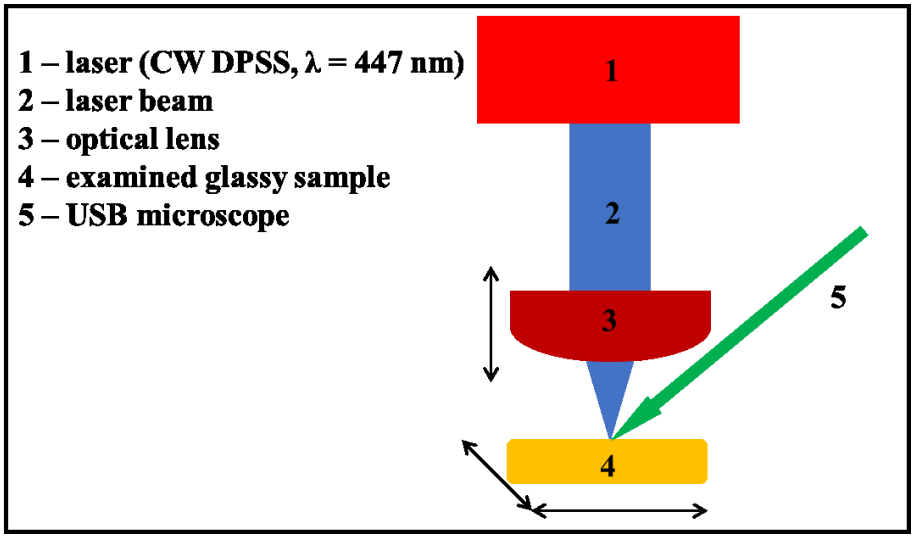

Fig. 1 *The simplified scheme of constructed optical apparatus used for the direct laser writing (CW diode-pumped solid state (DPSS) laser with λ = 447 nm) into the examined glasses.*

2.3 Measurement of photo-viscous changes

Photo-viscous changes were measured by penetration method using the thermomechanical analyzer TMA CX03RA-T (R.M.I., Czech Republic). For these purposes, the thermomechanical analyzer was modified (Fig. 2). For the laser beam passage, the top of the furnace was equipped with the optically transparent cup and hemispherical indenter was made from the optical quality silica glass. This experimental arrangement enables the simultaneous vertical illumination and force application in the same direction, both into the same place of the sample. The applicability of the modified TMA for the measurements by the penetration method was verified using the viscosity standard SRM 717a [37] in the temperature range 530-570 °C.

The photo-viscous changes were studied on the plan-parallel samples with thickness 1.0 ± 0.1 mm upon the illumination by λ = 405, 532, 650 and 808 nm with the laser power density in the range 1.0-2.2 W/cm^2. The measurements were performed at the temperatures slightly below glass transition temperature obtained from the dilatometric measurements. The time 540 min was selected to fulfill the condition for the applicability of the penetration method, i.e. penetration depth H << radius of indenter r_{ind} (1.02 mm) [38]. On the other hand, the viscosity value in the equilibrium state was not reached after the time 540 min. It was the reason why the viscous flow behavior was evaluated as the penetration rate of hemispherical indenter (v_{ind}^{dark} and v_{ind}^{ill} are the penetration rates for non-illuminated and illuminated samples, respectively).

The penetration rate was determined as the change of the volume of the hemispherical indenter (V) pushed into the sample surface per time unit in the time interval 200-480 min where the time dependence of V was constant.

The photo-viscous changes were finally evaluated/assessed by comparison of the penetration rates of illuminated and non-illuminated samples which both were measured at the same temperature.

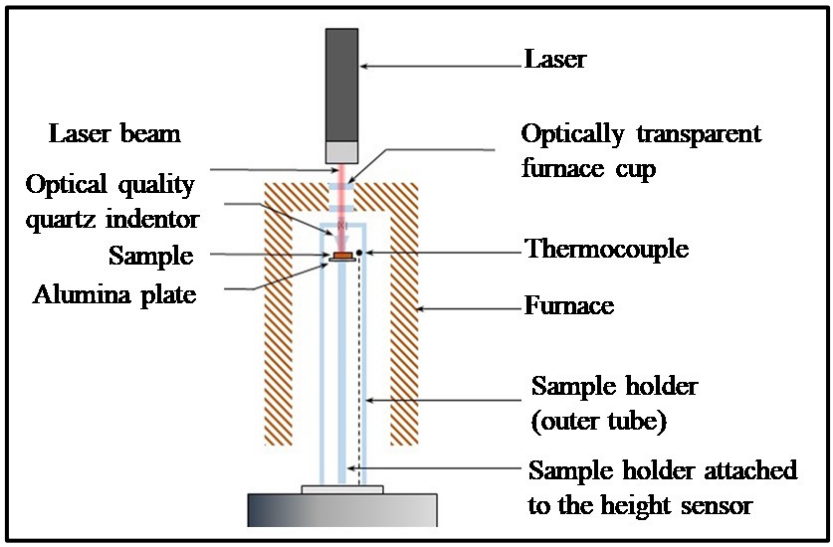

Fig. 2 *The simplified scheme of the modified measuring part of thermomechanical analyzer TMA CX03RA-T (R.M.I., Czech Republic) used for the measurements of photo-viscous changes in bulk glassy materials.*

2.4 Characterization of glasses and photo-induced effects

The prepared glasses were characterized by the various methods to obtain the information on their basic properties. The amorphous character of prepared glasses was verified using Roentgen diffraction analysis (XRD) by diffractometer D8 Advance (Bruker, USA). The information on the optical transmission of optically polished samples at the room temperature was obtained using UV/Vis spectroscopy (Lambda 20, Perkin Elmer, USA). The temperature dependence of optical transmission was measured by spectrophotometer HP UV-VIS 8453 equipped with the heating cell (Hewlett Packard, USA). In the case of PZPCo5 glass, the spectral dependence of diffuse reflectance was measured on powder sample due to the too high absorption of this composition using spectrophotometer Cintra 2020 (GBC, Australia).

The thermal properties such as glass transition temperature (T_g), heat capacity (c_p), crystallization temperature (T_c), melting point (T_m), softening temperature (T_s) and the coefficient of thermal expansion (CTE) in the temperature region 100-300 °C were determined employing Differential scanning calorimetry (Diamond, PerkinElmer, USA), Differential thermal analysis (DTA 03, R.M.I., Czech Republic) and Thermomechanical analysis (TMA CX04R, R.M.I., Czech Republic). The information on thermal conductivity of selected samples was obtained using LFA 457 (Netzsch, Germany).

The coordination and oxidation state of Co^{n+} ions present in some studied glasses were examined using the measurement of temperature dependence of magnetic

susceptibility by Gouy balance system equipped with the heating cell (Newport Instruments, Great Britain).

The photo-induced effects formed on the sample surfaces were characterized as well. The topography of created microobjects and also the topography of sample surfaces used for the determination of sample roughness were determined by Digital holographic microscope DHM R1000 (Lynceé Tec, Switzerland). In the case of microcraters with depth (d) beyond the DHM resolution (i.e. d > 10 μm), 3D Digital optical microscope VHX 6000 (Keyence, Japan) was used to measure their topography. Optical microscope BX 60 (Olympus, Japan) was employed to take images of non-illuminated surface and created microobjects and to verify the optical transmission and functionality of created microlenses.

Some properties of created microobjects were compared with the properties of non-illuminated samples. The structure of glasses and microobjects was examined by measurements of Raman spectroscopy using Dimension P2 (Lambda Solution, USA) emitting at 532 or 785 nm. The chemical composition of non-illuminated samples and created microobjects was obtained by EDX analysis (SEM JSM-5500LV equipped with the detector GRESHAM Sirius 10, Jeol, Japan). The mechanical properties (i.e. hardness) were compared by Nanoindentation (Hysitron TI 950, Hysitron, Netherlands).

To estimate the overheating of the spot on the sample surface illuminated during the direct laser writing, the thermal model was created using SW COMSOL Multiphysics 5.6. For the simulation of temperature rise during the illumination, the following material and laser properties and parameters were used: density obtained by Archimedean method, temperature dependences of thermal conductivity and heat capacity, optical penetration depth of used laser beam including its temperature dependence, cylindrical sample with diameter and thickness both 10 mm, laser beam diameter 180 μm with various laser power densities and the ambient temperature 300 K.

3. Results and discussion

3.1 Photo-induced formation of microlenses on the surface of PbO-Ga_2O_3 glasses

The prepared and characterized (i.e. thermal and optical properties) glasses from binary PbO-Ga_2O_3 system (PG1-PG5, see Table 1) were illuminated by CW laser emitting at 447 nm during the exposition times 0.1-60 s. The illumination led to the microlenses formation due to the photo-expansion. As the important parameter for the microlenses description, their height obtained by DHM was taken. The dependence of the microlenses height on the laser power density in a logarithmic scale was used to obtain the other important parameter characterizing the microlenses formation – the threshold power density of the microlenses formation ($F_{th,\ lens}$). This parameter was evaluated as the intersection of linear part of the mentioned dependence with x-axis [14] and was along with the microlenses height used to determine the role of various effects on the microlenses formation.

The maximal microlens height is not significantly affected by the chemical composition (Fig. 3). On the other hand, the parameter $F_{th,\ lens}$ is strongly affected by chemical composition of glass. The highest value of parameter $F_{th,\ lens}$ was observed for PG2 glass (74.7 mol% of PbO), see Fig. 3. The stable structure [31] consisting of metagallates and lead polyhedral chains is expected as the reason of the observed

PG2 glass response to the illumination. The structure of PG2 glass exhibits the equilibrium between these different chains in its structure which causes the highest thermal stability. The highest thermal stability should be given by the lowest value of fragility factor [31]. It was also found that the whole concentration dependence of $F_{th,\,lens}$ is in good agreement with the behavior of fragility factor (Fig. 3b).

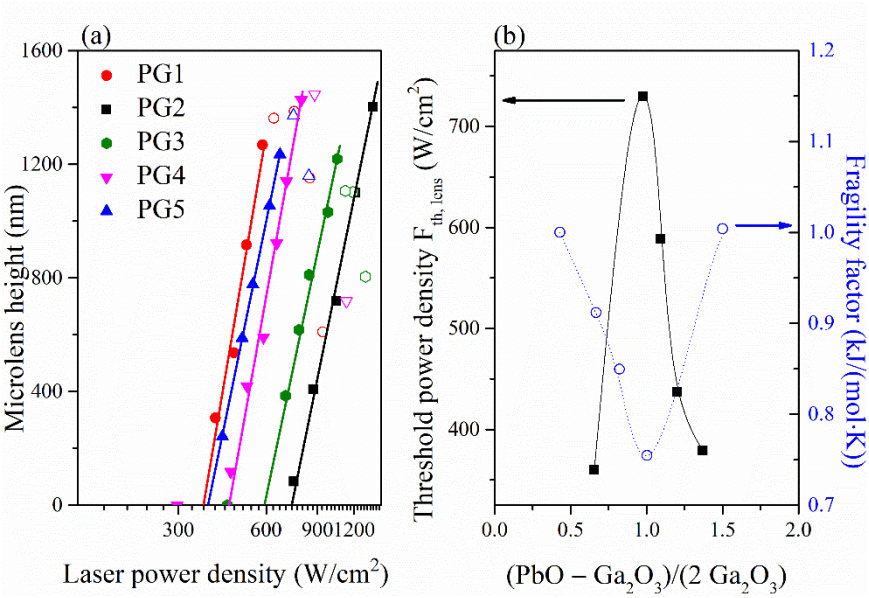

Fig. 3 *(a) The role of chemical composition on the microlenses formation in the glassy system PbO-Ga_2O_3 expressed by dependence of microlenses height on the laser power density for exposition time 0.5 s and (b) the comparison of $F_{th,\,lens}$ behavior depending on the chemical composition with the trend of fragility factor (data depicted from [31]). The lines are only to guide the eyes.*

The exposition time (0.1-60 s) and laser power density influence the microlenses formation as well, see Fig. 4. The microlenses height increases with the increase of both parameters to the certain maximal value. In the case of laser power density (F_L), the microlenses height increases linearly in the certain range of dependence h vs. ln F_L. At the higher values of F_L (e.g. for 5 s and PG2 above 1200 W/cm^2), the topography of microlenses is changed and the deviation from the linear part of dependence h vs. ln F_L occurs, see the empty squares in Fig. 4b. The reason for this behavior could be probably too high overheating, thermocapillary forces or partial crystallization [17].

The parameter $F_{th,\,lens}$ decreases with the increasing exposition time probably due to the increasing heat dissipation in a material, e.g. $F_{th,\,lens} \approx 1000$ W/cm^2 for 0.1 s and 660 W/cm^2 for 60 s illumination, respectively.

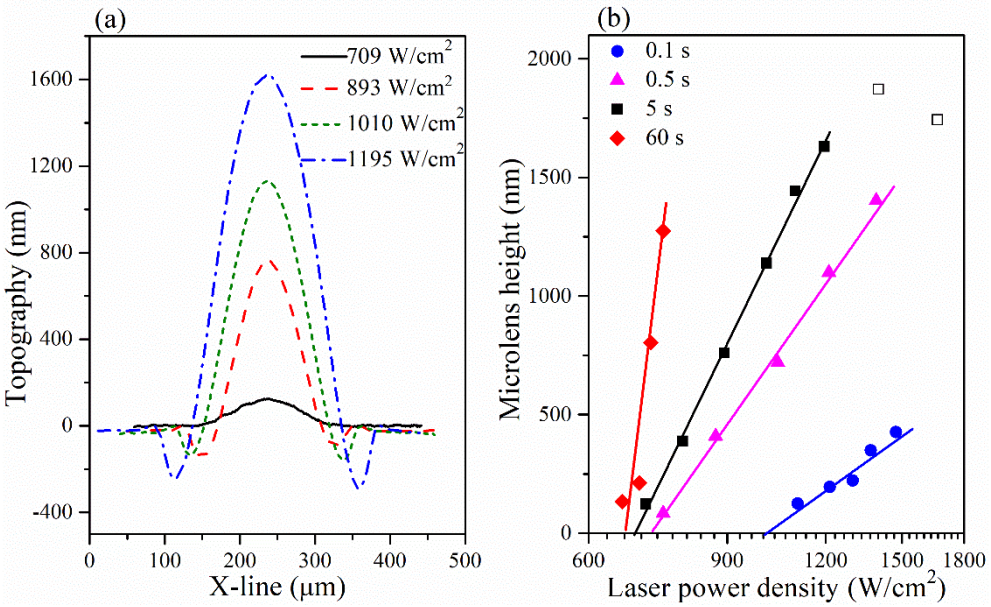

Fig. 4 *(a) 2D topographical profiles of microlenses created on the surface of PG2 glass using exposition time 5 s and various laser power densities and (b) the influence of exposition time (0.1-60 s) and laser power density on the microlenses formation (the empty squares correspond to the deviation of microlenses height from the linear trend).*

The overheating in the illuminated spot based on the measurement of temperature on the sample bottom side upon illumination, similarly as in [14], was estimated ≈ 550 °C in steady-state. The calculation of the theoretical maximal height of microlens using this overheating magnitude was in the good agreement with the maximal experimental obtained microlens height (1.80 μm vs. 1.87 μm, respectively). Based on the estimated overheating and the used experimental conditions, the local thermal expansion with the contribution of the self-focusing effect due to the large used laser power density (F_L = 1200 W/cm^2 corresponds to ≈ 37.7 kW/cm^3 for PG2 glass) is expected as the main mechanism causing the photo-induced formation of microlenses in the examined glassy system PbO-Ga_2O_3.

3.2 Photo-induced effects on the surface of PbO-Bi_2O_3-Ga_2O_3 glasses

As the second glassy system for the study of photo-induced effects, $(PbO)_{75-x}(Bi_2O_3)_x(Ga_2O_3)_{25}$, x = 0-29.8 mol% (PG2, PBG1-PBG5 in Table 1), was selected. Lead (II) oxide was partially replaced by bismuth (III) oxide - the role of Bi_2O_3 on the response of glasses to illumination was examined. The second reason was the toxicity of Pb-based compounds.

The photo-induced effects on the surface of prepared and characterized (density, thermal and optical properties) glasses were created using CW laser (λ = 447 nm, t = 0.5 s). The illumination by various laser power densities led to three different microobjects, see e.g. results obtained for glass with 7.6 mol% of Bi_2O_3 (PBG2) in Fig. 5. Firstly, at the low used laser power densities, no microobjects were observed (Region I). The higher laser power densities, i.e. ≈ 300-800 W/cm^2 in this case, led to the photo-expansion of illuminated spot of sample which resulted in the formation of microlenses (Region II). Subsequently, at laser power densities > 800 W/cm^2,

the illuminated spot of glass was probably more overheated which caused the formation of "dimple" microlenses (Region III) or microcraters (Region IV). The "dimple" microlenses are microlenses in which their center dropped down a little and thus the microlenses shape is deformed. In the case of microcraters formation, no photo-expansion proceeds but the material is removed from the illuminated spot during the illumination.

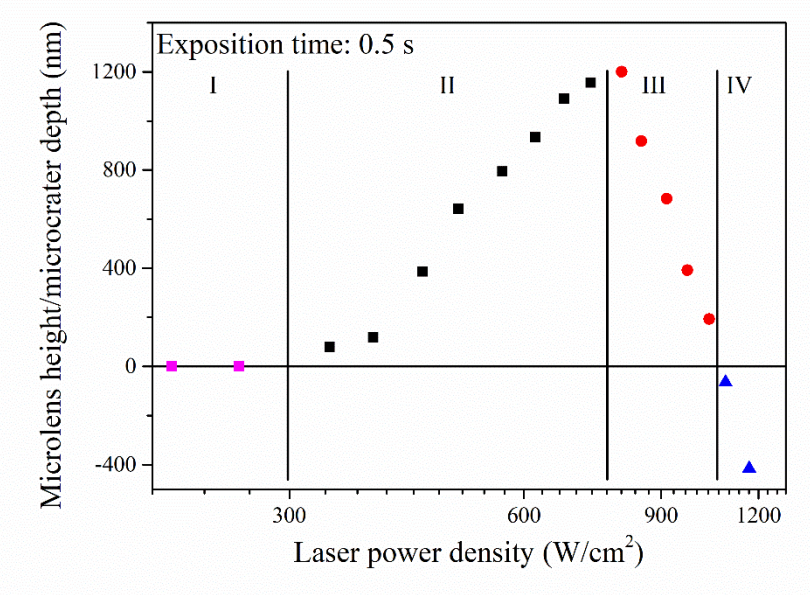

Fig. 5 *The typical material response in photo-induced changes of examined $PbO\text{-}Bi_2O_3\text{-}Ga_2O_3$ glasses (in this case PBG2) in dependence of microobject height/depth on the laser power density (the region I – no photo-induced effect, II – microlenses, III – "dimple" microlenses, IV – microcraters).*

To understand and explain the observed behavior and to estimate the overheating magnitude in the illuminated spot and in its surrounding, the thermal model was employed using the obtained physical parameters for glass with 7.6 mol% of Bi_2O_3.

In the case of microlenses formation (e.g. laser power density 600 and 800 W/cm^2), the overheating of the spot on the sample surface was calculated to be around temperature ≈ 300 and 350 °C (Fig. 6) which is slightly below corresponding glass transition temperature (T_g = 383 °C). It is therefore suggested as in case of glasses from binary $PbO\text{-}Ga_2O_3$ system that the mechanism of microlenses formation is the local thermal expansion of the overheated illuminated glass.

For the border of the "dimple" microlenses and microcraters formations – 1050 W/cm^2, the estimated overheating is ~ 420 °C (Fig. 6) which corresponds with the softening temperature of the studied PBG2 glass (T_s = 418 °C). It is suggested that "dimple" microlenses formation occurs due to the deformation of microlenses centers, by their own mass as the result of viscosity decrease. In the case of the microcraters creation, the increasing viscous flow and/or selective materials removal (based on the results obtained from EDX analysis described below) are assumed.

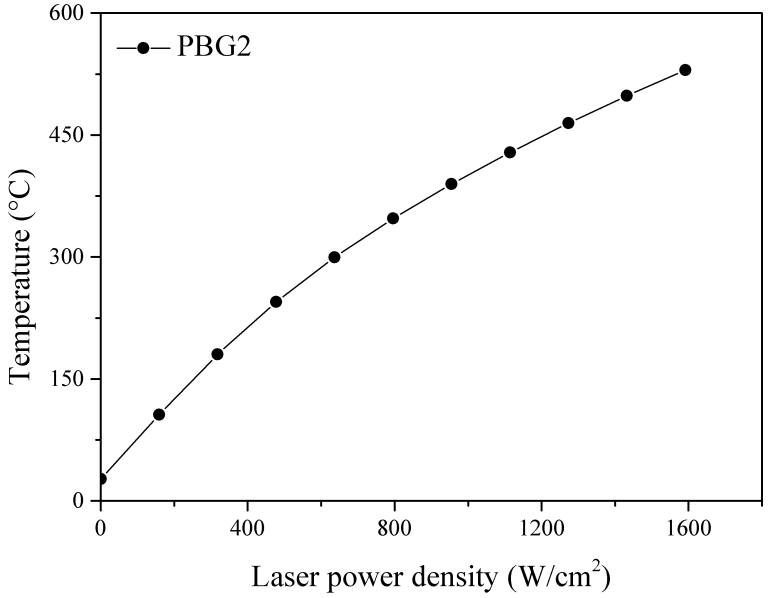

Fig. 6 *The calculated temperature rise in the center of the illuminated spot of PBG2 glass by CW laser beam emitting at 447 nm using the various laser power densities using the created thermal model.*

The role of Bi_2O_3 content on the microlenses formation was determined by the $F_{th,\ lens}$ parameter and is shown in Table 3. The value of this parameter decreased dramatically comparing to the glass without Bi_2O_3 (i.e. PG2). Furthermore, with the increasing Bi_2O_3 content, $F_{th,\ lens}$ value remains practically the same within the experimental error for glasses in the range 7.6-29.8 mol% of Bi_2O_3 (i.e. PBG2-PBG5). It is suggested that the glass transition temperature and optical penetration depth determine predominantly the $F_{th,\ lens}$ values in this case.

Table 3 *Important parameters influencing the threshold power density of microlenses formation ($F_{th,\ lens}$) in the ternary glassy PbO-Bi_2O_3-Ga_2O_3 system: the chemical composition and values of glass transition temperature (T_g) and optical penetration depth (d_p).*

Parameter\glass	PG2	PBG1	PBG2	PBG3	PBG4	PBG5
T_g (°C)	408	394	383	377	372	370
d_p (μm)	318	285	256	276	284	278
$F_{th,\ lens}$ (W/cm^2)	730	425	360	370	370	350

The created microlenses (region II in Fig. 5) were characterized and the results are described below. The radius of curvature (r_c) and focal length (f) were calculated for the highest created microlenses similarly as in [35]. The values of r_c and f increase with Bi_2O_3 content increase and are in the range 3.1-5.7 mm and 2.4-4.1 mm, respectively. The change of linear refractive index due to the formation of microlenses calculated according to the Lorentz-Lorenz relation [34] is almost the same for the glass without (74.7 mol% of PbO) and with Bi_2O_3 (e.g. 7.6 mol% of Bi_2O_3), i.e. $\Delta n_0 \approx$ -0.02-(-0.03). Furthermore, the functionality of microlenses for the potential application as passive optical element was verified by the successful imaging of the selected object through the microlens, see Fig. 7.

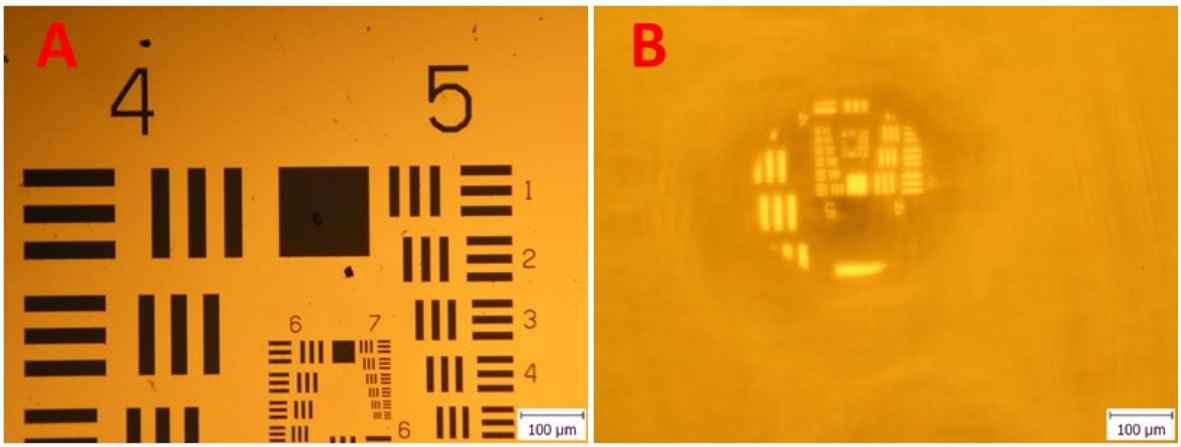

***Fig.** 7 USAF 1951 Resolution Target: (a) its image obtained by optical microscopy and (b) the imaging of its part through the microlens created on the surface of PBG2 glass (h = 1160 nm, F_L = 730 W/cm^2, exposition time 0.5 s, CW laser with λ = 447 nm). The same magnification 200x was used for both measurements.*

The selected properties of microlenses were compared with the properties of non-illuminated sample. No changes in the chemical composition and structure between the microlenses and non-illuminated surface using EDX analysis and Raman spectroscopy were observed. On the contrary, the nanoindentation hardness decreases for the microlens by ≈ 14 rel%.

The second effect manifesting in volume expansion, next to the microlenses, was microlines formation. The microlines were formed by the thermal expansion of overheated material during the simultaneous motion of sample and laser illumination. The height of the microlines was taken as the main parameter. The maximal obtained microlines height increased with the increasing Bi_2O_3 content (from 510 nm to 890 nm for binary PG2 and ternary PBG3 glass). The properties of microlines formed by the thermal expansion had the similar trends in behavior as the microlenses, i.e. no changes in the chemical composition and structure occurred during their formation and their nanoindentation hardness decreased compared to that for non-illuminated sample.

The microcraters formation was also examined in more detail. In this case, for CW laser (λ = 447 nm) the exposition time 60 s was used to reach the sufficient overheating of the illuminated surface. It was found, unlike microlenses, that the microcraters diameter is significantly affected by the laser power density. The microcraters diameter increases as well as their depth with the increasing laser power density. Therefore, both values of diameter and depth were used to determine the threshold power density of microcraters formation ($F_{th,\ crater}$), for example for binary glass with 74.7 mol% of PbO, see Fig. 8. Microcraters depth was used for the determination of $F_{th,\ crater}$ similarly as height in the case of microlenses, see e.g. [39]. In the case of microcraters diameter, the dependence of square value of microcraters diameter on the laser power density in the logarithmic scale was applied, see e.g. [40]. Both obtained values of $F_{th,\ crater}$ are very similar (i.e. 540 vs. 580 W/cm^2) in respect to the different way of their determination.

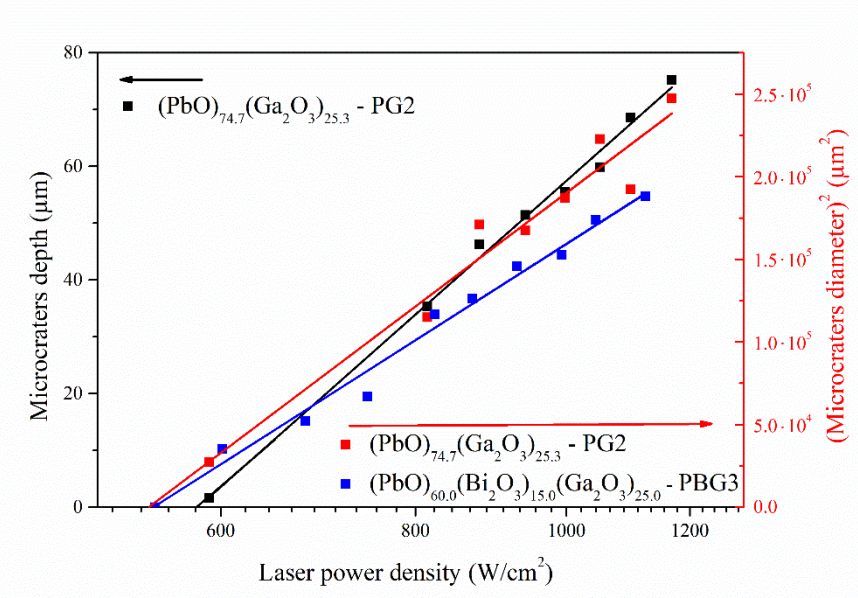

Fig. 8 *The dependences of the microcraters depth and diameter on the laser power density for glasses PG2 and PBG3. The lines were used for the determination of* $F_{th,\ crater}$.

The role of chemical composition on the microcraters formation was examined by comparison of binary glass with 74.7 mol% of PbO (PG2), i.e. without Bi_2O_3 content, with the ternary glass containing 15.0 mol% of Bi_2O_3 (PBG3). Nevertheless, the parameter $F_{th,\ crater}$ is not influenced by the change of chemical composition in this case. It is expected that the reason could be the similar optical and thermal properties of both glasses.

The created microcraters were characterized by EDX analysis. The chemical composition of the microcraters center was strongly changed due to the illumination. It was found that the intensity of Pb and/or Bi lines was significantly reduced. The obtained result seems to confirm the suggested mechanism of microcraters formation, i.e. selective removal of the lowest melted and/or volatile compounds. The same behavior was also observed for the microchannels, formed by the removal of the illuminated material during the sample motion.

3.3 Photo-induced effects on the surface of PbO-ZnO-CoO-P_2O_5 glasses

In the previous studied glassy systems, the photo-induced effects were caused by the absorption of the used light through the short wavelength absorption edge. In the next section of this work, the microlenses and microcraters formations induced by a different absorption mechanism, i.e. by the colour centers – ions Co^{2+}, were examined upon the illumination using CW laser with $\lambda = 532$ nm for 60 s.

The prepared glasses were firstly characterized from point of important properties. The oxidation state of Co^{2+} ions was confirmed by the magnetic susceptibility measurement. Based on the value of effective magnetic moment, the present Co^{2+} ions are high-spin octahedrally coordinated. The spectral dependence of diffuse reflectance and assignment of the deconvoluted absorption bands to the individual electronic transitions by Tanabe-Sugano diagrams [41] were used to obtain the information on the optical properties. The values of optical penetration depth, coefficient of thermal

expansion and glass transition temperature were determined to explain the role of chemical composition on the glass response to the illumination.

The illumination by CW laser with λ = 532 nm for 60 s led to the formation of microlenses and microcraters on the surface of two glasses with the highest Co^{2+} ions content, i.e. 2.02 and 3.57 mol% of CoO only. On the surface of glasses with lower Co^{2+} ions content, no photo-induced changes were observed after the illumination probably due to the low absorption resulting in the low overheating of the illuminated surface.

It was found that the highest microlenses were created on the surface of glass with 2.02 mol% of CoO (PZPCo4), i.e. $h_{max} \approx 1440$ nm (Table 4). On the other hand, glass with the highest CoO content (3.57 mol%, PZPCo5) exhibits the lower value of $F_{th, lens}$ by ~ 21 rel% compared to PZPCo4 glass. It is assumed that the reason of observed behavior could be the almost twice higher value of optical penetration depth for glass PZPCo4 while maintaining similar values of thermal properties, i.e. glass transition temperature and coefficient of thermal expansion. The created microlenses on the surface of PZPCo4 glass were characterized by calculation of refractive index change [34], radius of curvature and focal length [35]. All obtained characteristics reach the values of similar order as in the case of binary and ternary glasses.

Table 4 *The parameters used for the comparison of the microobjects formation on the surface of glasses PZPCo4 and PZPCo5: glass transition temperature (T_g), optical penetration depth of λ = 532 nm (d_p), the threshold power densities of microlenses ($F_{th, lens}$) and microcraters formation ($F_{th, crater}$) and maximal obtained microlenses height (h_{max}) and microcraters depth (d_{max}).*

Parameter\Glass	PZPCo4	PZPCo5
T_g (°C)	374	383
d_p (μm)	360	200
CTE (ppm/K)	14.7	14.8
$F_{th, lens}$ (W/cm^2)	240	190
h_{max} (nm)	1440	770
$F_{th, crater}$ (W/cm^2)	375	290
d_{max} (nm)	760	740

The formation of microcraters was also compared for the two above-mentioned glasses. The maximal detected depths of microcraters were practically the same for both glasses. On the other hand, the value of $F_{th, crater}$ is influenced by Co^{2+} ions content. $F_{th, crater}$ value was lower for the glass with higher Co^{2+} ions content, i.e. PZPCo5, (Table 4). It is different behavior in comparison with glasses from binary $PbO\text{-}Ga_2O_3$ and ternary $PbO\text{-}Bi_2O_3\text{-}Ga_2O_3$ systems where the $F_{th, crater}$ values do not depend on the chemical composition. In this case, the reason could be probably the different absorption mechanism, significantly different optical penetration depth and distance between Co^{2+} ions present in glasses.

3.4 Photo-viscous changes in selected glasses with the different mechanism of optical absorption

In the last part of this work, the photo-viscous changes in three different glasses with the different structure and/or absorption mechanisms (i.e. chalcogenide glass As_2S_3

and phosphate glasses without Co^{2+} ions (PZPCo0) and with the concentration of CoO ~ 3.57 mol% (PZPCo5)) were examined by the penetration method using the modified thermomechanical analyzer. The advantage of the modified thermomechanical analyzer is the application of both mechanical force and laser light into the same place on the sample and both act in the same direction. The photo-viscous changes were studied especially due to the assumption that they could be connected with the formation of microobjects on the surface of some glasses [25].

The chalcogenide bulk glass As_2S_3 was selected as the model material to determine the basic parameters influencing the photo-viscous changes and to compare the obtained results with the literature, e.g. [25, 27]. It is assumed that the photon energy could influence the photo-viscous changes. Based on the optical properties of As_2S_3 slightly below its glass transition temperature ($E^{03} \approx 2.25$ eV for T = 178 °C), four wavelengths λ = 405, 532, 650 and 808 nm absorbed in the various regions of short wavelength absorption edge were selected. It was found that each of used wavelengths led to the increase of penetration rate of optically transparent indenter at T = 178 °C (T_g from TMA ≈ 202 °C).

The wavelengths λ = 532, 650 and 808 nm cause the real increase of penetration rate of used indenter, i.e. the real photo-viscous changes. The highest photo-viscous changes at the same measured temperature 178 °C were observed for the wavelength 650 nm (Table 5) which is absorbed in the Urbach region of short wavelength absorption edge. It is suggested that the reason could be the optimal absorption coefficient determining the optical penetration depth which is in this case comparable with the thickness of the examined samples. Furthermore, the used wavelength 650 nm has probably the ideal sub-band gap photon energy which is suitable for the disruption of weak binding interactions and/or formation of charge defects [25, 26, 42] which both could increase the mobility of atoms and/or clusters.

On the other hand, in the case of λ = 405 nm, the increase of penetration rate was only apparent, since the detected penetration depth of indenter was affected by the formation of concentric circles around the measuring point on the glassy surface. It was assumed that this effect is connected with the breaking and subsequent photo-oxidation of As-S bonds [43, 44] during the interaction of As_2S_3 and photons with high energy (i.e. > 2.7 eV, λ = 405 nm corresponds to photon energy 3.06 eV). The products of photo-oxidation (As_4O_6, S_2 [43]) are probably immediately removed from the sample during the used experimental conditions.

Table 5 *The properties of used lasers (wavelength (λ) and photon energy (E^{ph})) and parameters used for the assessment of size of the photo-viscous changes in bulk As_2S_3 glass (penetration rates for non-illuminated (v_{ind}^{dark}) and illuminated samples (v_{ind}^{ill}) and their ratio $v_{ind}^{ill}/v_{ind}^{dark}$) at T = 178 °C.*

λ (nm)	**E^{ph} (eV)**	**v_{ind}^{dark}; v_{ind}^{ill} (μm³/min)**	**$v_{ind}^{ill}/v_{ind}^{dark}$ (-)**
Non-illuminated	-	890	-
405	3.06	3690*	4.1*
532	2.33	1890	2.1
650	1.91	5370	6.0
808	1.53	1530	1.7

*apparent photo-viscous change affected by photo-oxidation of surface

The influence of laser power density (0.3-2.2 W/cm^2) was investigated still at the same temperature 178 °C using 650 nm illumination. It was found that the penetration rate of indenter (affected by the viscous flow) increased with the increase of laser power density. The threshold power density of photo-viscous changes is equal to ≈ 0.2 W/cm^2 for As_2S_3 at T = 178 °C.

To find out if the effect of illumination is transient or permanent, the cyclic measurements (alternation of steps in the dark and with illumination) of the viscous flow were done. Fig. 9 clearly shows that the photo-induced increase of viscous flow is only temporary. After the finishing of the illumination it immediately vanishes and the viscous flow almost returns to the original state, i.e. to the state before the illumination (i.e. "dark").

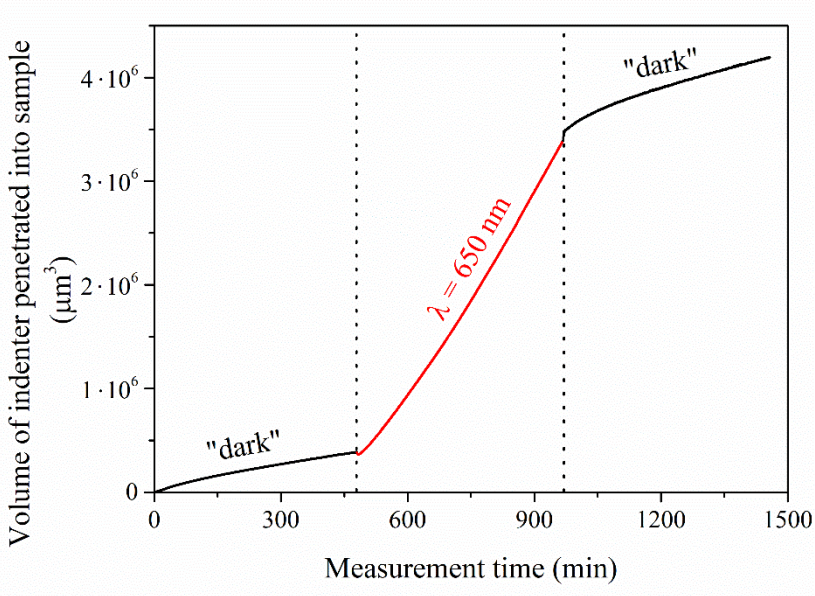

Fig. 9 *The cyclic measurement of photo-viscous changes, i.e. dark – illumination – dark in bulk As_2S_3 upon 650 nm illumination at T = 178 °C (applied force 500 mN).*

The role of different temperatures of measurement on the photo-viscous changes was examined as well since the viscous flow exhibits significant temperature dependence [45, 46]. It was found that the illumination causes the higher penetration rate of indenter in comparison with the non-illuminated conditions for the all same measured temperatures (Fig. 10). On the other hand, the size of the observed photo-viscous changes expressed as $v_{ind}^{ill}/v_{ind}^{dark}$ decreases with the increasing temperature and possesses the monotonous dependence. It is assumed that two reasons or their combination can induce the observed photo-viscous changes. The first is the local temperature rise in the illuminated spot which could be estimated from the shift of the penetration rates upon illumination to higher values. This shift is estimated to be approximately 7 °C for temperature of measurement 178 °C. The second reason described in literature [25-27] assumes that the various athermal photo-structural changes can occur in As_2S_3 and they are the cause of the observed photo-viscous changes. Nevertheless, in this work the presence of the suggested photo-structural changes was not confirmed nor refused using available experimental methods.

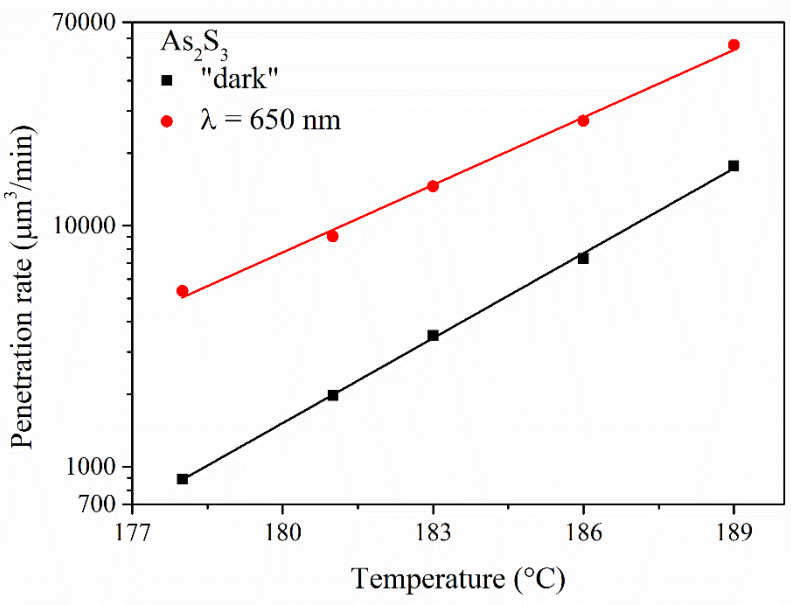

Fig. 10 *The temperature dependences of penetration rates for non-illuminated (black cubes) and illuminated (red circles) samples of bulk As_2S_3 glass.*

The photo-viscous changes were also studied in selected phosphate glasses - sample without Co^{2+} ions (PZPCo0) and with Co^{2+} ions (PZPCo5). The cyclic measurements of viscous flow were performed using 650 nm illumination (Fig. 11). It is clearly seen, as expected, that no photo-viscous changes were observed in glass without Co^{2+} ions since light with λ = 650 nm was not absorbed. Contrary to it, the presence of Co^{2+} ions led to the successful increase of viscous flow due to the illumination. This increase, similarly as in As_2S_3, immediately vanishes after the finishing of the illumination. In addition, due to the photon energy significantly lower than the optical band gap of PZPCo5 glass (short wavelength absorption edge is located in UV region) and energy of the present covalent bonds, the local temperature rise without any structural changes is suggested as the reason of photo-viscous changes.

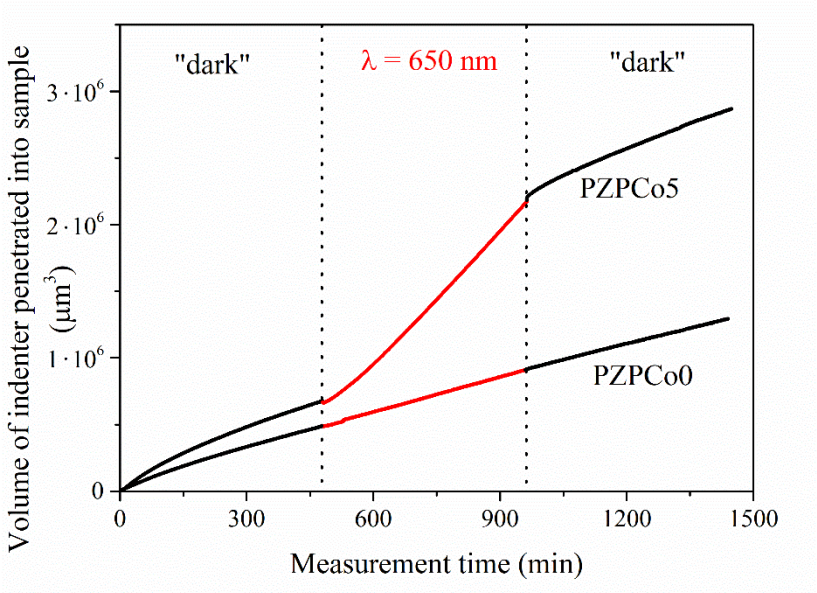

Fig. 11 *The cyclic measurements of photo-viscous changes (i.e. dark – illumination – dark) for sample without Co^{2+} ions (PZPCo0) and with Co^{2+} ions (PZPCo5).*

The role of photon energy/wavelength and temperature on the photo-viscous changes was examined for glass containing Co^{2+} ions as well. The effect of wavelength was studied using three different laser sources (λ = 532, 650 and 808 nm). The illumination by λ = 808 nm practically does not induce the photo-viscous changes since this wavelength is not absorbed by Co^{2+} ions. The wavelengths λ = 532 and 650 nm caused the increase of penetration rates and the highest changes were observed using 650 nm illumination (the ratio $v_{ind}^{ill}/v_{ind}^{dark}$ equals to 4.0 and 1.5 for λ = 650 and 532 nm, respectively). It is suggested that the reason of the observed behavior could be the type of the individual electronic transitions at the used wavelengths. It is assumed that spin-forbidden transitions could be relaxed by a heat production, but some of spin-allowed transitions could lead to a radiative relaxation process. Hence, only the intensity of spin-forbidden transitions was taken to explain the observed behavior. The spin-forbidden transition $^2E \leftarrow {}^4T_{1g}$ detected at λ = 650 nm is more intensive compared to spin-forbidden transition $^2T_2/^2T_1 \leftarrow {}^4T_{1g}$ observed at λ = 532 nm which results probably in higher local temperature rise leading to higher penetration rate for λ = 650 nm.

The role of temperature on the photo-viscous changes in PZPCo5 glass was not so significant as in case of As_2S_3. The penetration rate due to the illumination by 650 nm was higher than that for non-illuminated sample, but the slopes of both temperature dependences of penetration rates for illuminated and non-illuminated sample are practically the same within the experimental error (Fig. 12). It is assumed that this effect could be connected with the different absorption mechanisms in studied glasses (i.e. by absorption bands due to d-d transitions of Co^{2+} ions in phosphate glass and by short wavelength absorption edge in As_2S_3) and/or with the different nature of observed photo-viscous changes (the contribution of some photo-structural changes to photo-viscous changes is also considered in As_2S_3).

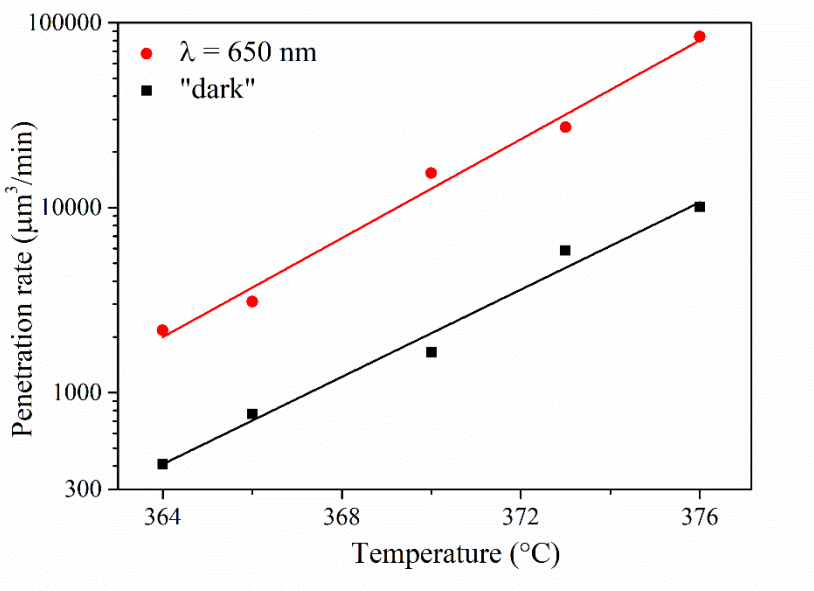

Fig. 12 *The role of temperature of measurements on the penetration rates during measurements without (black cubes) and with illumination (red circles) in PZPCo5 glass.*

4. Conclusion

This dissertation thesis was focused on photo-induced effects (microlenses, microlines and microcraters) created on the surface of high-refractive index glasses by continuous-wave (CW) lasers (λ = 447 and 532 nm depending on the optical properties of glasses). Three different glassy systems were selected, i.e. $PbO\text{-}Ga_2O_3$, $PbO\text{-}Bi_2O_3\text{-}Ga_2O_3$ and $PbO\text{-}ZnO\text{-}CoO\text{-}P_2O_5$. All glasses were prepared by melt-quenching technique on the air and the surfaces were polished to the optical quality. Properties of illuminated and non-illuminated surface areas were compared. The modified thermomechanical analyzer was used to confirm influence of viscous flow on the microobjects creation.

The microobjects were created by the volume expansion (convex microlenses, microlines) and by the material removal (microcraters). Microlenses were formed on the surface of glasses at the lowest used laser power densities and/or exposition times. As the main parameters characterizing their formation, the microlenses height and the threshold power density of microlenses formation ($F_{th,\ lens}$) were used. It was found that the microlenses formation depends mainly on the laser power density, exposition time and also on the chemical composition/structure of glass.

Convex microlenses were characterized also from the point of their imaging properties (potential applications). The functionality of convex microlenses for imaging applications was verified by the displaying of the selected object through a microlens. The change of linear refractive index of formed microlenses calculated according to Lorentz-Lorenz relation was approximately the same for all studied glasses ($\Delta n_0 \approx$ -0.03). The focal length of the highest created microlenses was order of millimeters.

The microlines were prepared on the surface of $PbO\text{-}Bi_2O_3\text{-}Ga_2O_3$ system by the motion of the samples in x-axis during the illumination. The maximal height of microlines increased with the increase of Bi_2O_3 content up to 890 nm for glass with 15.0 mol% of Bi_2O_3.

The created microlenses and microlines were characterized by EDX, Raman spectroscopy and nanoindentation. No changes in the chemical composition and structure and on the other hand, the decrease of nanoindentation hardness of both microlenses and microlines in comparison with non-illuminated surface were observed. Based on the above-mentioned results and used thermal model, the nature of these microobjects formation is the thermal expansion of local overheated material.

When the longer exposition time and/or higher laser power density of the corresponding CW laser were used, the material was locally removal from illuminated spot and microcraters were created. The microcraters depth and their diameter were taken as basic parameters for their characterization. The value of $F_{th,crater}$ did not depend on the chemical composition for both binary and ternary glasses since these glasses have similar optical and thermal properties. On the other hand, in the case of $PbO\text{-}ZnO\text{-}CoO\text{-}P_2O_5$ glasses, the $F_{th,\ crater}$ value was influenced by Co^{2+} ions content due to the significant difference in optical penetration depth. It is suggested based on the thermal model and EDX analysis that the microcraters are formed in these studied systems due to the increasing viscous flow followed by the selective removal of the lowest melted or volatile compounds.

It was found that the photo-induced formation of microobjects on the glassy surfaces strongly depends on viscous flow of material upon the illumination. The viscous flow and its photo-induced changes were therefore measured by modified thermomechanical analyzer which allows the action of force and illumination in the same direction on the same place of the sample. For these purposes, glasses with different structure and even with the different light absorption mechanisms were selected (As_2S_3 and oxide glass with Co^{2+} ions).

It was observed that the illumination causes the higher penetration rate of TMA indenter compared to the non-illuminated conditions at the same temperature. The role of basic parameters influencing photo-viscous changes such as photon energy, laser power density and temperature was determined.

The cyclic measurements of viscous flow (dark 1 – illumination – dark 2) show that the viscous flow increases temporary upon illumination, its increase immediately vanishes when the laser is switched off and the penetration rate (dark 2) has a very similar value as before illumination, i.e. dark 1.

It is assumed that the nature of the photo-viscous changes can be different in the studied glasses. The local temperature rise, photo-structural changes or their combination are suggested as the reason of photo-viscous changes in As_2S_3. In the case of oxide glass with Co^{2+} ions, the local temperature rise is suggested as the mechanism.

This study extended the microstructuring of glassy surfaces by CW lasers into high-refractive index oxide glasses. Obtained data could contribute to the better understanding of the mechanism of formation of microobject on the surface of glasses.

5. List of references

[1]. FRUMAR, M., B. FRUMAROVA, T. WAGNER a P. NEMEC. Photo-Induced Phenomena in Amorphous and Glassy Chalcogenides. In: A.V. Kolobov. *Photo-induced metastability in amorphous semiconductors*. Cambridge: Wiley-VCH, 2003, s. 23-44. ISBN 3527403701.

[2]. TICHÝ, L., H. TICHÁ, P. NAGELS a E. SLEECKX. A review of the specific role of oxygen in irreversible photo- and thermally induced changes of the optical properties of thin film amorphous chalcogenides. *Optical Materials*. 1995, **4** (6) 771-779. ISSN 0925-3467.

[3]. KUTÁLEK, P. a L. TICHÝ. On the thickness dependence of both the optical band gap and reversible photodarkening in amorphous Ge-Se films. *Thin Solid Films*. 2016, **619** 336-341. ISSN 0040-6090.

[4]. KINCL, M., J. TASSEVA, K. PETKOV, P. KNOTEK a L. TICHY. On the photo-induced shift of the optical gap in amorphous $Ge_6As_{43}S_{35}Se_{16}$ film. *Journal of Optoelectronics and Advanced Materials*. 2009, **11** (4) 395-398. ISSN 1454-4164.

[5]. IIJIMA, M. a S. KURITA. Transient photoinduced phenomena in amorphous chalcogenide thin films. *Journal of Applied Physics*. 1980, **51** (4) 2103-2105. ISSN 0021-8979.

[6]. TANAKA, K., T. NAKAGAWA a A. ODAJIMA. Photodarkening in glassy chalcogenide systems. *Philosophical Magazine B*. 1986, **54** (1) L3-L7. ISSN 1364-2812.

[7]. KNOTEK, P., L. TICHY, D. ARSOVA, Z.G. IVANOVA a H. TICHA. Irreversible photobleaching, photorefraction and photoexpansion in GeS_2 amorphous film. *Materials Chemistry and Physics*. 2010, **119** (1) 315-318. ISSN 0254-0584.

[8]. LIVINGSTON, F.E., P.M. ADAMS a H. HELVAJIAN. Examination of the laser-induced variations in the chemical etch rate of a photosensitive glass ceramic. *Applied Physics A*. 2007, **89** (1) 97-107. ISSN 1432-0630.

[9]. KOMATSU, T. a T. HONMA. Laser patterning and growth mechanism of orientation designed crystals in oxide glasses: A review. *Journal of Solid State Chemistry*. 2019, **275** 210-222. ISSN 0022-4596.
[10]. KOLOBOV, A. a J. TOMINAGA. Chalcogenide glasses as prospective materials for optical memories and optical data storage. *Journal of Materials Science: Materials in Electronics*. 2003, **14** 677-680. ISSN 0957-4522.
[11]. SAVASTRU, D., S. MICLOS a R. SAVASTRU. Infrared chalcogenide microlenses. *Journal of Optoelectronics and Advanced Materials*. 2006, **8** (3) 1165-1172. ISSN 1454-4164.
[12]. DONGOL, R., L. TWEETON, C. FARIS, S. FELLER a M. AFFATIGATO. Mechanisms of Laser Induced Modification of Lead and Barium Vanadate Glasses. *Journal of Applied Physics*. 2011, **109** 013521. ISSN 0021-8979.
[13]. KUTÁLEK, P., P. KNOTEK, A. ŠANDOVÁ, T. VACULOVIČ, E. ČERNOŠKOVÁ a L. TICHÝ. Ablation of binary As_2S_3, As_2Se_3, GeS_2, $GeSe_2$ and $GeSe_3$ bulk glasses and thin films with a deep ultraviolet nanosecond laser. *Applied Surface Science*. 2021, **554** 149582. ISSN 0169-4332.
[14]. KNOTEK, P. a L. TICHY. On photo-expansion and microlens formation in $(GeS_2)_{0.74}(Sb_2S_3)_{0.26}$ chalcogenide glass. *Materials Research Bulletin*. 2012, **47** (12) 4246-4251. ISSN 0025-5408.
[15]. HISAKUNI, H. a K. TANAKA. Giant Photoexpansion in As_2S_3 Glass. *Applied Physics Letters*. 1994, **65** (23) 2925-2927. ISSN 0003-6951.
[16]. BEADIE, G., W.S. RABINOVICH, J. SANGHERA a I. AGGARWAL. Fabrication of microlenses in bulk chalcogenide glass. *Optics Communications*. 1998, **152** (4-6) 215-220. ISSN 0030-4018.
[17]. ANDREETA, M.R.B., L.S. CUNHA, L.F. VALES, L.C. CARASCHI a R.G. JASINEVICIUS. Bidimensional codes recorded on an oxide glass surface using a continuous wave CO_2 laser. *Journal of Micromechanics and Microengineering*. 2011, **21** (2) 025004. ISSN 0960-1317.
[18]. DELGADO, T., D. NIETO a M.T. FLORES-ARIAS. Fabrication of microlens arrays on soda-lime glass using a laser direct-write technique and a thermal treatment assisted by a CO_2 laser. *Optics and Lasers in Engineering*. 2015, **73** 1-6. ISSN 0143-8166.
[19]. KIM, T.H., Y.S. KIM, Y.J. JEONG, Y.H. NA, H.S. YOON, J.J. KIM a B.K. RYU. Micromachining of transition metal ion doped glass surface by using a pulsed Nd:YAG (532 nm) laser for the optical device. *Current Applied Physics*. 2009, **9** (3, Supplement) S234-S236. ISSN 1567-1739.
[20]. SMUK, A.Y. a N.M. LAWANDY. Direct laser fabrication of dense microlens arrays in semiconductor-doped glass. *Journal of Applied Physics*. 2000, **87** (8) 4026-4030. ISSN 0021-8979.
[21]. ANTONOV, I., F. BASS, Y. KAGANOVSKII, M. ROSENBLUH a A. LIPOVSKII. Fabrication of microlenses in Ag-doped glasses by a focused continuous wave laser beam. *Journal of Applied Physics*. 2003, **93** (5) 2343-2348. ISSN 0021-8979.
[22]. HISAKUNI, H. a K. TANAKA. Optical fabrication of microlenses in chalcogenide glasses. *Optics letters*. 1995, **20** (9) 958-960. ISSN 1539-4794.
[23]. MESSADDEQ, S.H., V.R. MASTELARO, M. SIU LI, M. TABACKNIKS, D. LEZAL, A. RAMOS a Y. MESSADDEQ. The influence of oxygen in the photoexpansion of GaGeS glasses. *Applied Surface Science*. 2003, **205** (1) 143-150. ISSN 0169-4332.
[24]. KNOTEK, P. a L. TICHY. Explosive boiling of $Ge_{35}Sb_{10}S_{55}$ glass induced by a CW laser. *Materials Research Bulletin*. 2013, **48** (9) 3268-3273. ISSN 0025-5408.
[25]. TANAKA, K. Photoinduced fluidity in chalcogenide glasses. *Comptes Rendus Chimie*. 2002, **5** (11) 805-811. ISSN 1631-0748.

[26]. REPKA, M., M. FRUMAR a M. HRDLICKA. Photo-induced change of viscosity of glassy selenium below its glass transition temperature. *Journal of Physics and Chemistry of Solids*. 2007, **68** (5) 940-942. ISSN 0022-3697.
[27]. TAGANTSEV, D. a S. NEMILOV. Photoviscosity effect in chalcogenide glasses. *Soviet Journal of Glass Physics and Chemistry (od 1993, Glass Physics and Chemistry)*. 1989, **15** 220-231. ISSN 0360-5043.
[28]. TICHÁ, H., J. SCHWARZ, L. TICHÝ a R. MERTENS. Physical Properties of PbO-ZnO-P_2O_5 Glasses II. Refractive Index and Optical Properties. *Journal of Optoelectronics and Advanced Materials*. 2004, **6** (3) 747–753. ISSN 1454-4164.
[29]. HEO, J. a C.Z. QUAN. Photo-Induced Effect in Heavy Metal Oxide Glasses. *Journal of the American Ceramic Society*. 2010, **93** (4) 913-914. ISSN 0002-7820.
[30]. DUMBAUGH, W.H. a J.C. LAPP. Heavy-Metal Oxide Glasses. *Journal of the American Ceramic Society*. 1992, **75** (9) 2315-2326. ISSN 0002-7820.
[31]. JEWELL, J.M. a J.A. RULLER. A structural model for PbO-Ga_2O_3-SiO_2 glasses. *Journal of Non-Crystalline Solids*. 1993, **152** (2) 179-187. ISSN 0022-3093.
[32]. SHELBY, J.E. Lead Galliate Glasses. *Journal of the American Ceramic Society*. 1988, **71** (5) C-254-C-256. ISSN 0002-7820.
[33]. LIU, H.S., T.S. CHIN a S.W. YUNG. FTIR and XPS studies of low-melting PbO-ZnO-P_2O_5 glasses. *Materials Chemistry and Physics*. 1997, **50** (1) 1–10. ISSN 0254-0584.
[34]. KRAGH, H. Ludvig Lorenz and nineteenth century optical theory: the work of agreat Danish scientist. *Applied Optics*. 1991, **30** (33) 4688-4695. ISSN 0003-6935.
[35]. SANCHEZ, E.A., M. WALDMANN a C.B. ARNOLD. Chalcogenide glass microlenses by inkjet printing. *Applied Optics*. 2011, **50** (14) 1974-1978. ISSN 0003-6935.
[36]. BACH, H. a N. NEUROTH. *The Properties of Optical Glass*. New York: Springer Berlin Heidelberg, 1998. 414 s. ISBN 9783642577697.
[37]. Certificate Standard Reference Material 717a, NATIONAL INSTITUTE OF STANDARDS & TECHNOLOGY, Gaithersburg 2018. Dostupné z: https://www-s.nist.gov/srmors/certificates/717A.pdf.
[38]. MÁLEK, J. a J. SHÁNĚLOVÁ. Viscosity of germanium sulfide melts. *Journal of Non-Crystalline Solids*. 1999, **243** (2) 116-122. ISSN 0022-3093.
[39]. BEN-YAKAR, A. a R.L. BYER. Femtosecond laser ablation properties of borosilicate glass. *Journal of Applied Physics*. 2004, **96** (9) 5316-5323. ISSN 0021-8979.
[40]. HERTWIG, A., S. MARTIN, J. KRÜGER a W. KAUTEK. Interaction area dependence of the ablation threshold of ion-doped glass. *Thin Solid Films*. 2004, **453-454** 527-530. ISSN 0040-6090.
[41]. COTTON, F.A. a G. WILKINSON. *Anorganická chemie: Souborné zpracování pro pokročilé.* Praha: ACADEMIA, 1973. 1102 s.
[42]. FRITZSCHE, H. Photo-induced fluidity of chalcogenide glasses. *Solid State Communications*. 1996, **99** (3) 153-155. ISSN 0038-1098.
[43]. JANAI, M., S. OSCAR, S.G. LIPSON a P.S. RUDMAN. Image evaluation of the light-enhanced vaporization photolithographic process in As_2S_3 thin films. *Optics letters*. 1978, **2** (2) 51-53. ISSN 0146-9592.
[44]. TANAKA, K. Spectral dependence of photoexpansion in As_2S_3 glass. *Philosophical Magazine Letters*. 1999, **79** (1) 25-30. ISSN 0950-0839.
[45]. KOŠŤÁL, P., J. SHÁNĚLOVÁ a J. MÁLEK. Viscosity of chalcogenide glass-formers. *International Materials Reviews*. 2019, **65** (2) 63-101. ISSN 0950-6608.
[46]. ANGELL, C. Thermodynamic Aspects of the Glass Transition in Liquids and Plastic Crystals. *Pure and Applied Chemistry*. 1991, **63** (10) 1387-1392. ISSN 1365-3075.

List of Student's Published Works

Impact Factor Journals

[1] SMOLÍK, J., P. KNOTEK, J. SCHWARZ, E. ČERNOŠKOVÁ, P. KUTÁLEK, V. KRÁLOVÁ a L. TICHÝ. Laser direct writing into PbO-Ga_2O_3 glassy system: Parameters influencing microlenses formation. *Applied Surface Science*. 2021, **540** (1) 148368. ISSN 0169-4332.

[2] SMOLÍK, J., P. KNOTEK, J. SCHWARZ, E. ČERNOŠKOVÁ, P. JANÍČEK, K. MELÁNOVÁ, L. ZÁRYBNICKÁ, M. POUZAR, P. KUTÁLEK, J. STANĚK, J. EDLMAN a L. TICHÝ. 3D micro-structuring by CW direct laser writing on PbO-Bi_2O_3-Ga_2O_3 glass. *Applied Surface Science*. 2022, **589** 152993. ISSN 0169-4332.

[3] SMOLÍK, J., E. ČERNOŠKOVÁ, P. KNOTEK, Z. ZMRHALOVÁ, J. SCHWARZ, Z. ČERNOŠEK a T. PLECHÁČEK. Viscous flow changes induced by illumination in selected chalcogenide and phosphate glasses detected by thermomechanical analysis. *Journal of Non-Crystalline Solids* – v recenzním řízení (manuskript NOC-S-22-00859).

Impact Factor Journals – other articles

[1] KNOTEK, P., T. PLECHÁČEK, J. SMOLÍK, P. KUTÁLEK, F. DVOŘÁK, M. VLČEK, J. NAVRÁTIL a Č. DRAŠAR. Kelvin probe force microscopy of the nanoscale electrical surface potential barrier of metal/semiconductor interfaces in ambient atmosphere. *Beilstein Journal of Nanotechnology*. 2019, **10** (10) 1401-1411. ISSN: 2190-4286.

[2] HRUŠKA, B., A. NOWICKA, M. CHROMČÍKOVÁ, E. GREINER-WRONA, J. SMOLÍK, V. SOLTÉZS a M. LIŠKA. Raman spectroscopic study of corroded historical glass. *International Journal of Applied Glass Science*. 2021, **12** (4) 613-620. ISSN: 2041-1294.

[3] KUTÁLEK, P., P. KNOTEK, P. JANÍČEK, R. TODOROV, E. ČERNOŠKOVÁ, J. SMOLÍK, A. ATANASOVA a L. TICHÝ. Photo-induced solid-state reaction on the interface of As_2S_3–$Ge_{30}Se_{70}$ thin films. *Optical Materials*. **123** 111897. ISSN: 0925-3467.

Non-Impact Peer-Reviewed Journals

[1] SMOLÍK, J., P. KNOTEK, J. SCHWARZ, P. KUTÁLEK, M. POUZAR a E. ČERNOŠKOVÁ. Optimization of synthesis and basic characterization of 55PbO-10ZnO-35P_2O_5 glass modified by CoO. *Scientific Papers of the University of Pardubice, Series A; Faculty of Chemical Technology*. 2020, **26** 181–193. ISSN 1211-5541.

[2] SMOLÍK, J., Z. ZMRHALOVÁ, P. KNOTEK, E. ČERNOŠKOVÁ a T. PLECHÁČEK. Thermomechanical analysis as a useful tool to study photoinduced changes of the viscous flow of glassy materials. *Scientific Papers of the University of Pardubice, Series A; Faculty of Chemical Technology*. 2021, **27** 137–149. ISSN 1211-5541.

Conference Talks

[1] SMOLÍK, J., P. KNOTEK, P. KUTÁLEK, J. SCHWARZ a E. ČERNOŠKOVÁ. Fotoindukovaná tvorba mikročoček v oxidických sklech systému PbO-Ga_2O_3 a PbO-Ga_2O_3-Bi_2O_3. Anorganické nekovové materiály – odborný seminář doktorandů, Praha (Česká republika), 6.–7. 2. 2019.

[2] SMOLÍK, J., P. KNOTEK, P. KUTÁLEK, J. SCHWARZ a E. ČERNOŠKOVÁ, Photoinduced Expansion of PbO-Based Heavy Metal Oxide Glasses. 7th International Conference on Chemical Technology (ICCT), Mikulov (Česká republika), 15.–17. 4. 2019, ISBN: 978-80-88307-01-3.

[3] SMOLÍK, J., J. SCHWARZ, P. KUTÁLEK, P. KNOTEK, J. STANĚK a E. ČERNOŠKOVÁ. Different photoinduced effects in Heavy Metal Oxide Glass. 71. ZJAZD CHEMIKOV, Vysoké Tatry (Slovensko), 9.–13. 9. 2019.

[4] SMOLÍK, J., P. KNOTEK, J. SCHWARZ, P. KUTÁLEK a E. ČERNOŠKOVÁ. From glassy lenses to microlenses. 21. celoslovenská študentská vedecká konferencia s medzinárodnou účasťou - Chémia a technológie pre život, Bratislava (Slovensko), 6. 11. 2019, ISBN 978-80-8208-015-8.
[5] SMOLÍK, J., Z. ZMRHALOVÁ, P. KNOTEK, J. SCHWARZ, L. TICHÝ a E. ČERNOŠKOVÁ. Změny viskózního toku skel vlivem osvitu. Anorganické nekovové materiály - XXVI. ročník odborného semináře doktorandů, Praha – virtuální forma (Česká republika), 24.–25. 2. 2021.
[6] SMOLÍK, J., P. KNOTEK, J. SCHWARZ, J. STANĚK, P. KUTÁLEK, L. TICHÝ a E. ČERNOŠKOVÁ. Direct laser writing on the surface of $PbO\text{-}Bi_2O_3\text{-}Ga_2O_3$ glasses. 8th International Conference on Chemical Technology (ICCT), Praha – virtuální forma (Česká republika), 3.–5. 5. 2021, ISBN: 978-80-88214-24-3.

Conference Posters

[1] SMOLÍK, J., P. KNOTEK, P. KUTÁLEK, J. SCHWARZ a E. ČERNOŠKOVÁ. Laser direct writing to the $PbO\text{-}Ga_2O_3$ glasses. Summer School ELISS 2019, Dolní Břežany (Česká republika), 25.–30. 8. 2019.
[2] SMOLÍK, J., J. SCHWARZ, P. KNOTEK, P. KUTÁLEK a E. ČERNOŠKOVÁ. Direct laser writing to the PbO-rich phosphate glasses modified by CoO. 9th EPS-QEOD EUROPHOTON VIRTUAL CONFERENCE, Praha – virtuální forma (Česká republika), 30. 8.–4. 9. 2020.
[3] SMOLÍK, J., Z. ZMRHALOVÁ, P. KNOTEK, E. ČERNOŠKOVÁ, J. SCHWARZ a L. TICHÝ. TMA measurements of the viscous flow changes in glasses induced by illumination. 14th International Conference on Solid State Chemistry (SSC 2020), Trenčín – virtuální forma (Slovensko), 14.–17. 6. 2021, ISBN 978-80-8075-947-6.

Other contributions

[1] STANĚK, J., E. ČERNOŠKOVÁ, J. SCHWARZ, J. SMOLÍK, M. VLČEK a P. KNOTEK. Fotoindukovaná tvorba kráterů v $PbO\text{-}Ga_2O_3$ skle. *Sborník příspěvků: studentská vědecká odborná činnost 2018/2019*. Pardubice: Univerzita Pardubice, 2019. ISBN 978-80-7560-260-2.
[2] KNOTEK, P., J. SMOLÍK, E. ČERNOŠKOVÁ, L. TICHÝ a P. KUTÁLEK. Ablation of chalcogenide bulk glasses and thin films with a deep ultraviolet nanosecond laser. Conference on Materials and Nanomaterials, Paříž (Francie), 17.–19. 7. 2019, přednáška.
[3] KUTÁLEK, P., P. KNOTEK, A. ŠANDOVÁ, J. SMOLÍK, L. TICHÝ a T. VACULOVIČ. Ablation of binary chalcogenide glasses by UV ns laser. 17th International Conference of Nanosciences & Nanotechnologies (NN20), Thessaloniki (Řecko), 7.–10. 7. 2020, přednáška.
[4] KNOTEK, P., J. SMOLÍK, E. ČERNOŠKOVÁ, J. SCHWARZ, P. JANÍČEK, P. KUTÁLEK, J. STANĚK, J. EDLMAN a L. TICHÝ. The effect of Bi_2O_3 content on micro-lens, -craters and waveguide formation in $PbO\text{-}Bi_2O_3\text{-}Ga_2O_3$ glasses by direct laser writing. The 22nd International Symposium on Laser Precision Microfabrication (LPM2021), Hirosaki, Aomori – virtuální forma (Japonsko), 8.–11. 6. 2021, přednáška.
[5] KOPECKÁ, K., J. SCHWARZ, J. SMOLÍK a P. KNOTEK. Využití mikrovln pro slinování smaltů. *Sborník příspěvků: studentská vědecká odborná činnost 2021/2022*. Pardubice: Univerzita Pardubice, termín obhajoby 13. 6. 2022.
[6] KNOTEK, P., J. SMOLÍK, J. SCHWARZ a E. ČERNOŠKOVÁ. Different approaches for determination of hardness changes in micro-structured glasses. Nanobrücken: Nanomechanical Testing Conference. Praha (Česká republika), 8.–10. 6. 2022, poster.